JOURNAL OF MATERIALS SCIENCE 12 (1977) 2223–2234

Experimental determination of some periclase and spinel compositions in the system $CaO-MgO-Al_2O_3-Cr_2O_3-Fe-O_2-SiO_2$

G. M. BIGGAR
Department of Geology, University of Edinburgh, West Mains Road, Edinburgh, UK

The solubilities of Cr_2O_3, Fe_2O_3 and Al_2O_3 (as well as CaO and SiO_2) in periclase were determined from samples equilibrated in the temperature range 1550 to 1725° C, at two oxygen pressures (air and fO_2 about 10^{-9} atm). Most samples contained periclase, spinel, and liquid which is the mineralogy of most chrome-bearing refractories at manufacturing and service temperatures. In air a large observed change in the R_2O_3 (where $R_2O_3 = Al_2O_3 + Fe_2O_3 + Cr_2O_3$) content of periclase with increasing temperature results in a new example of retrograde solubility which causes crystalline periclase to grow in amount in some refractory compositions as the temperature increases. At low oxygen fugacity ($\log fO_2 \sim -9$) the iron oxide content (mainly FeO) of the periclase decreased (from 6.4 to 1.3 wt %) as temperature increased. In air the iron oxide content ($FeO + Fe_2O_3$) decreased marginally (typically from 6.8 to 6.4 wt %) as temperature increased which contrasts with previous literature statements that there is an increase. At both oxygen pressures the Cr_2O_3 content increases markedly as temperature increases (up to 17 wt %), suggesting that Cr_2O_3 (and not Fe_2O_3 as the previous literature states) may be the cause of textural changes observed in commerical products subjected to temperature cycling. The presence of increasing CaO in the bulk samples leads to lower R_2O_3 contents in the periclase crystals. The data allow further more restricted choices to be made in refractory formulations towards the goal of matching the phase compositions to the properties desired at service temperatures. A few analyses of spinels show that iron levels decrease as temperatures increase and CaO levels up to 0.9 wt % were encountered.

1. Introduction

The individual solubilities of each of Al_2O_3, Cr_2O_3, FeO, Fe_2O_3, CaO in crystalline MgO in appropriate binary systems, such as $MgO–Al_2O_3$, $MgO–Cr_2O_3$, etc, have been known for years, but data for the simultaneous solubility of several of these oxides in MgO in ternary and higher systems are sparse. A review [1] of the available data for the quaternary system $CaO–MgO–Al_2O_3–SiO_2$ was in fact based almost entirely on results from ternary systems. Data are presented here for parts of the system $CaO–MgO–Al_2O_3–Cr_2O_3–Fe–O_2–SiO_2$ and some of its subsystems.

2. Experimental methods

A variety of starting materials (see below) was used and each composition was raised to, and held for up to 24 h at, temperatures from 1550 to 1725° C. In air, platinum capsules were used and at low oxygen fugacity molybdenum wire loops [2] were used. All samples were quenched into water and the product partially crushed and examined in transmitted light, in reflected light, and by electron probe microanalyser to determine the phases present, and their compositions. A few reversal experiments were performed by holding products of high temperature runs at a lower tem-

TABLE I The compositions studied (molar proportions)

Code*	SiO_2	Al_2O_3	Cr_2O_3	Fe_2O_3	CaO	MgO	Code*	SiO_2	Al_2O_3	Cr_2O_3	Fe_2O_3	CaO	MgO
G 18	9	1			3	18	M 24A	4	1			12	25.33
G 4	4	1			3	9	M 24K	4	0.5	0.5		12	25.33
G 3	3	1			3	6	M 24F	4	0.25	0.5	0.25	12	25.33
G 2.5	2.5	1			3	3	M 7A	2.1	1			0.45	14.83
G 1	1	1			3	1	M 7K	2.1	0.5	0.5		0.45	14.83
GM 0.8	0.83	1			3	4	M 7F	2.1	0.25	0.5	0.25	0.45	14.83
M 8A	1.36	1			15	25.33	M 4K	2	1.5	1.5		1	24
M 8K	1.36	0.5	0.5		15	25.33	M 4F	2	0.75	1.5	0.75	1	24
M 8F	1.36	0.25	0.5	0.25	15	25.33	M 6K	1	3	3		2	45
M 16A	2.72	1			13.5	25.33	M 6F	1	1.5	3	1.5	2	45
M 16K	2.72	0.5	0.5		13.5	25.33	M 9K	1	7.5	7.5		5	105
M 16F	2.72	0.25	0.5	0.25	13.5	25.33	M 9F	1	3.75	7.5	3.75	5	105

*G signifies gel[2]. M signifies mixed oxides. GM signifies a gel with some MgO added. The numeral part of the code appears in Fig. 1. A signifies Al_2O_3. K signifies 50% Al_2O_3, 50% Cr_2O_3. F signifies 50% Cr_2O_3, 25% Al_2O_3 and 25% Fe_2O_3.

perature. The solubility levels thus obtained were mostly similar, and textural differences are discussed later.

Three types of starting materials were used; (i) gels [3] with compositons in the plane $Ca_3Al_2Mg_nSi_yO_z$ and for which phase equilibria up to 1580° C are known [4]; (ii) mixtures of the above gels and Analar MgO; (iii) oxide mixtures, CaO, Cr_2O_3, MgO, Al_2O_3, Fe_2O_3, SiO_2, compounded from respectively, Analar $CaCO_3$, $NH_4Cr_2O_7$, MgO, Al_2O_3; spectrographically pure, <50 ppm, Fe_2O_3; and SiO_2 from hydrolysed tetraethyl-ortho-silicate).

The 'gel' samples were carefully prepared using highest purity reagents [3] but probe analyses emphasize the problem of contamination. Samples prepared before 1970, before Cr_2O_3 and iron had been used in the laboratory, had low or undetectable contents of Cr_2O_3 (0.000 and 0.002%) and iron (up to 0.04%). Later samples (e.g. Table II) show Cr_2O_3 contents up to 0.4% in the liquid portion of a sample which probably implies about 0.2% in the bulk samples and iron levels up to 0.4%. Visible (pale green) contamination of chrome-free samples was believed to come from the furnace brickwork during sintering of mixed oxide samples. Additionally, a single batch of experiments at 1620° C revealed on analysis a variable and mysterious contamination of up to 2% Fe_2O_3. In retrospect, this accident was not the calamity it was originally thought to be and, indeed, the analytical data from the samples demonstrate that the solubility of elements in MgO are only a little affected by small changes in the levels of other elements present.

The products of the runs contained; (i) equilibrium crystals up to 200 μm in diameter, grown from starting materials with particles in general no larger than 20 μm; (ii) glass; (iii) fibrous or skeletal crystalline patches representing former liquid which had failed to freeze to a glass. Microprobe analyses of equilibrium crystals were satisfactory and duplicates, or triplicates, from the same experiment agreed closely. Analytical totals for periclase were in the range 99.3 to 101.0%. Analyses of homogeneous isotropic glasses were reasonably satisfactory with totals from 98.3 to 99.9% which is usual for silicate glasses. Analyses were attempted on some of the quench patches representing former liquid with hopeless results suggesting variability of this material at the micron level.

A routine analytical technique was followed and, although levels below 0.10 wt % are quoted in the tables, this is only to indicate that the element was looked for in the analyses and no reliance is claimed for values below 0.10%.

2.1. Compositions studies

The sample compositions are given in Table I. In many cases simple molar ratios for CaO, Al_2O_3, SiO_2 etc were chosen. In such complex systems a simplification is required to ease the discussion and the presentation of diagrams. The chosen method was to sum the molar quantities of Cr_2O_3, Al_2O_3, and Fe_2O_3 and call the total R_2O_3. The relative amounts of CaO, SiO_2 and R_2O_3 are recalculated in wt % as if moles of R_2O_3 were moles of Al_2O_3 and used to plot ternary diagrams. Thus, Fig. 1b is in effect a projection from MgO into the plane CaO–SiO_2–R_2O_3. Some samples

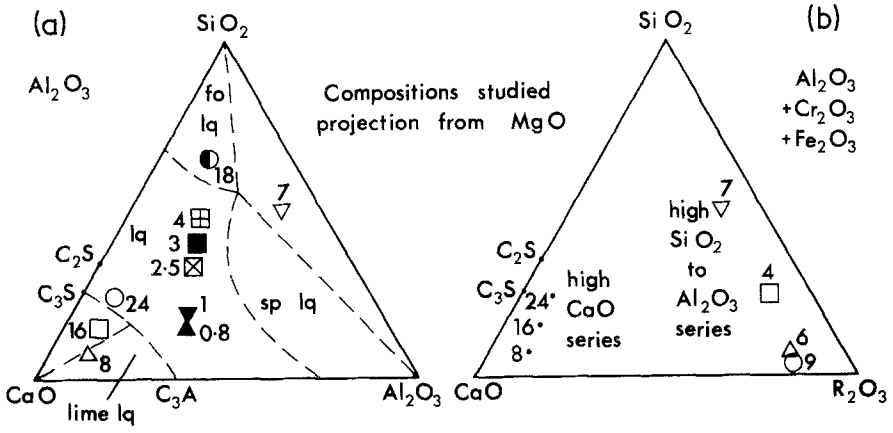

Figure 1 (a) The samples studied (Table I) seen in projection from MgO on to $CaO-Al_2O_3-SiO_2$. The symbols identify the samples from which the periclase analyses in Figs. 2a, b and c are derived and the numbers identify the chemical compositions in Table I. The results are discussed in Section 3. The dashed lines (Fig. 9, [4]) represent the likely form of the phase diagram at about 1600° C when R_2O_3 is Al_2O_3. (b) Samples with Cr_2O_3 and Fe_2O_3 plotted on to $CaO-R_2O_3-SiO_2$; in later figures the same symbols are used to identify compositions. Results for the high-SiO_2 to Al_2O_3 series are presented in Sections 4.1 and 4.2, and for the high-CaO series in Section 4.4.

TABLE II Probe analyses of periclase lime and glass in the system $CaO-MgO-Al_2O_3-SiO_2$

Comp.	(°C)*	SiO_2	Al_2O_3	Cr_2O_3†	Fe_2O_3†	CaO	MgO	Total	Others‡
7A	1725	0.05	3.84	0.51	0.33	0.05	94.86	99.64	None
7A	1690	0.10	3.45	0.11	0.15	0.02	05.46	99.29	None
7A	1650	0.03	2.62	0.16	0.24	0.06	96.50	99.60	None
7A	1620	0.03	2.32	0.01	0.62	0.03	96.61	99.68	Fo, Sp
7A	1560	0.01	1.64	0.01	0.08	0.05	97.81	99.61	Fo, Sp
18	1549	0.06	1.52	–	–	0.09	98.37	100.04	Fo
18	1549	0.05	1.47	–	–	0.13	98.77	100.41	Fo
4	1545	0.04	1.54	–	–	0.08	98.32	99.99	Sp
2.5	1545	0.01	1.49	–	–	0.13	98.56	100.91	Sp
2.5	1500	0.02	1.58	–	–	0.11	98.43	100.14	Sp
1	1500	0.04	0.66	–	–	0.26	99.20	100.16	None
24A	1690	0.01	0.23	0.01	0.00	1.05	98.58	99.89	Plus
24A	1620	0.00	0.28	0.00	0.21	0.91	98.60	100.00	Plus
24A	1560	0.02	0.37	0.01	0.01	0.72	99.04	100.17	Plus
8A	1690	0.01	0.28	0.04	0.23	1.28	98.26	100.09	L, plus
18	1690	0.09	1.10	0.16	0.25	0.05	97.60	99.25	Fo
3	1690	0.06	1.89	0.17	0.14	0.13	97.40	99.79	None
0.8	1690	0.05	0.87	0.06	0.04	0.51	98.61	100.13	None
1	1500	15.51	27.95	–	–	46.75	8.80	99.01	None
2.5	1498	31.15	15.67	–	–	34.66	18.25	99.73	Sp
0.8	1690	13.16	27.41	0.07	0.33	45.85	11.97	98.79	None
3	1690	30.19	16.84	0.02	0.24	27.90	24.75	99.94	None
8A	1690	12.52	21.69	0.39	2.52	55.95	5.17	98.25	L, plus
2.5	1545	28.87	18.74	–	–	32.61	19.57	99.79	Sp
8A	1690	0.00	0.03	0.00	0.13	95.09	3.82	99.08	L, plus
24A	1690	32.72	1.22	0.09	0.00	63.60	1.07	98.71	Plus

*The duration of experiments in this table and Table III was as follows: 1725° C for 20 h; 1690° C for 18 h; 1650° C for 19 h; 1620° C for 17 h; 1570° C for 18 h; 1560° C for 23 h; 1549° C for 5 h; 1545° C for 2 h; and 1500° for 4 h;
†These elements are contaminants. Values recorded as 0.00 indicate a result of less than 0.005% and a dash indicates that no X-ray counts were made for the element concerned.
‡This column indicates phases present in addition to periclase and liquid; "plus" implies unidentified silicates, probably dicalcium or tricalcium silicate; Fo is forsterite; Sp is spinel; L is lime.

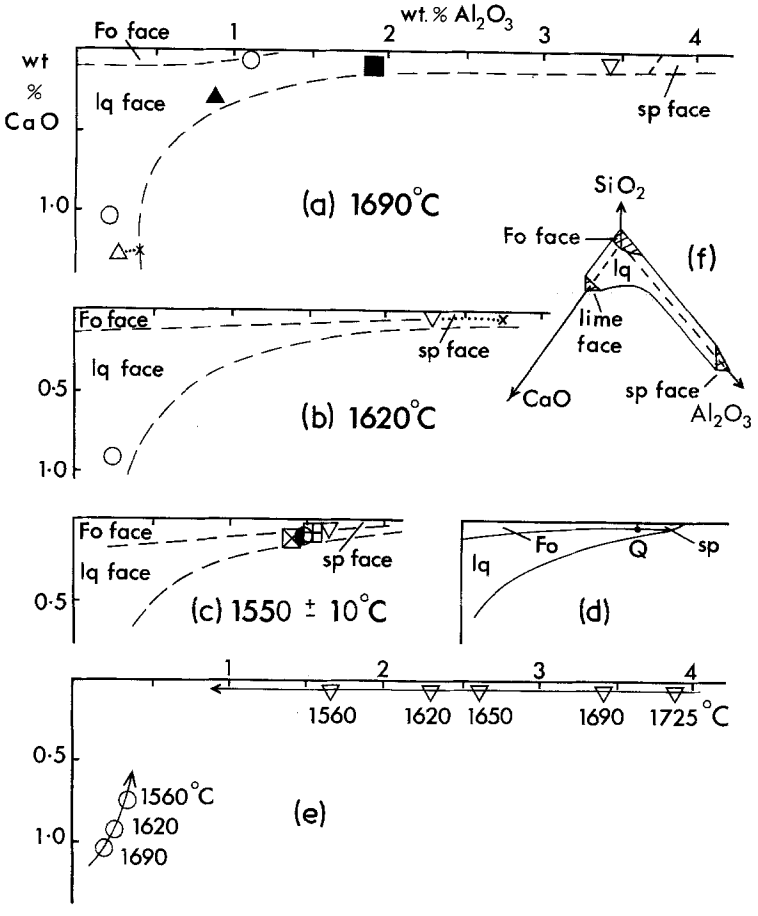

Figure 2 The Al_2O_3 and CaO contents of periclase compositions crystallized from samples in the system $CaO–MgO–Al_2O_3–SiO_2$ (the symbols identify the bulk compositions using Fig. 1a and Table I). Symbols linked by dotted lines to small crosses indicate the typical effect of calculating impurity Fe_2O_3 (data from Table II) as if it were a molar equivalent of Al_2O_3. Dashed lines are deduced possible positions of some of the faces of the periclase polyhedron. (a), (b) and (c) are isothermal and (d) is diagrammatic to indicate the manner in which the Fo, Sp and liquid faces of the periclase polyhedron probably join (in (b) and (c). (e) shows for each of two selected bulk compositions the locus of movement of the equilibrium periclase composition with temperature. For the composition 7A (▽), the section of the locus, below 1620° C is the locus of point Q being the apex of the periclase polyhedron at which the spinel forsterite and liquid faces meet. (f) is a 3-dimensional sketch.

(Fig. 1a) contained only Al_2O_3 in the R_2O_3 group; some contained equal molar amounts of Cr_2O_3 and Al_2O_3 (R_2O_3 = 50% Cr_2O_3 + 50% Al_2O_3); and some contained R_2O_3 in the mol % 50 Cr_2O_3 + 25 Al_2O_3 + 25 Fe_2O_3, which is close to the range found in commercial chrome-bearing refractories [5].

3. Results in the system $CaO–Al_2O_3–MgO–SiO_2$

In general, these samples were observed to contain the phases expected (Figs. 9 and 10 of [6]). Analyses of the periclase crystals gave a consistent series of analyses (Table II) from which Fig. 2a to e were constructed, to illustrate the movements of various faces of the periclase polyhedron [1]. Although little of the data is critical in defining accurately the extent of these faces, the dashed lines (and Fig. 2d) indicate the manner in which some of the faces may meet. For example at 1690° C the spinel and forsterite faces do not meet and the spinel face is not encountered in the present series of compositions but its presence is indicated. At 1550° C, samples containg Fo Per 1q, those containing Sp Per 1q, and those containing Fo Sp Per 1q have essentially the same periclase compositions, which must accordingly be the periclase composition at the apex of the periclase polyhedron at which the spinel, forsterite, and liquid faces meet (point Q, Fig. 2d). In detail the four analyses at 1560° C are in the wrong order to give a unique solution, the analytical techniques being beyond their limit of distinguishing similar compositions.

Liquids from the field of periclase plus liquid often quenched to a glass and were successfully analysed (Table II). Liquids from fields containing forsterite, or di- of tricalcium silicate, or lime, generally devitrified and the 'quench texture' give probe analyses which could not represent former liquid. The glass analyses are plotted in Fig. 3 in projection from MgO and are seen (i) to correspond closely to the projection of the original composition, or (ii) to lie on a tie-line from spinel through the original composition, or (iii) to lie at the apex

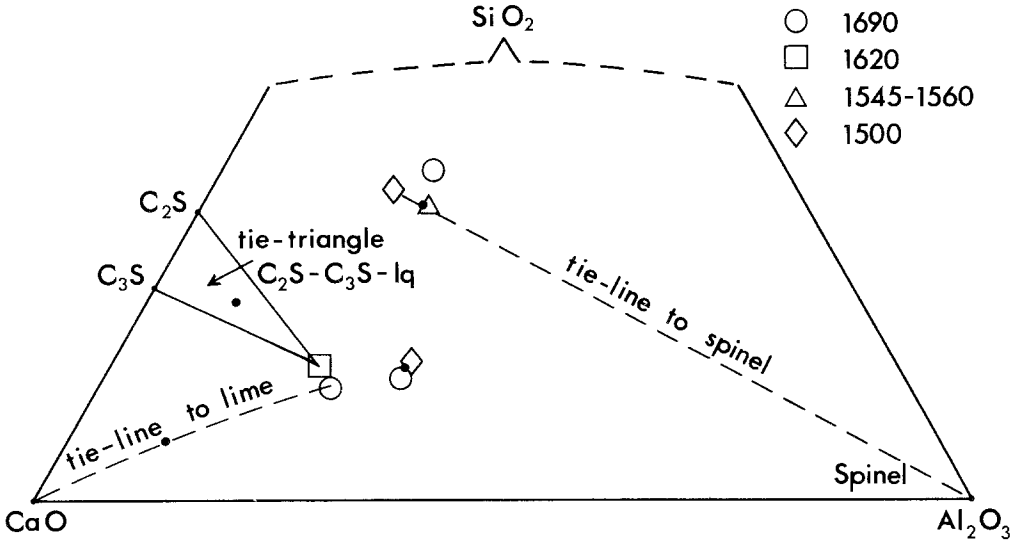

Figure 3 Glass analyses from samples containing periclase crystals projected from MgO into $CaO-Al_2O_3-SiO_2$. Original bulk compositions shown as small dots. Tie-lines (or tie-triangles) shown as appropriate when crystalline phases in addition to periclase are present. These data indicate that analyses of glasses which are free of quench effects are probably reliable guides to the composition of the former liquid (c.f. [7]).

of a tie-triangle. Some of the problems of accepting glass analyses as representative of former liquids have been discussed [7].

The CaO-rich compositions at some temperatures contained crystals which were probably C_3S and C_2S, but it was not obvious if these were primary or produced during the quench and they have not yet been further investigated except that their presence is reported in Table II by the word 'plus'. One analysis of a lime crystal quenched from 1690° C showed 3.8% MgO in solid solution and a crystal of dicalcium silicate showed 1.22% Al_2O_3 and 1.07% MgO (Table II).

The combination of glass and crystal analyses (Table II and Fig. 3) in principle allows accurate calculation of the percentage of each crystalline phase and the percentage of liquid present in a refractory composition at working temperature, but the limited data so far do not do more than confirm some of the provisional values of liquid contents (Figs. 9 to 11 of [6]).

4. Periclase solid solutions in systems with Cr_2O_3 and Fe_2O_3 present

Two groups of samples were studied (Fig. 1b); a high CaO group (Samples, 8, 16, 24) which often crystallized periclase with lime, or tricalcium silicate, or dicalcium silicate; and a group ranging from a high SiO_2 member (Sample 7) via Samples 4 and 6 to a high R_2O_3 member (Sample 9). Members of this group crystallized periclase usually with spinel and sometimes with forsterite. For all samples the phases present in each experiment are listed (Table III and IV). Each of the above groups was further extended in that in one series of samples R_2O_3 was composed of equimolar amounts of Al_2O_3 and Cr_2O_3 and a second series had R_2O_3 composed of 50% Cr_2O_3 + 25% Al_2O_3 + 25% Fe_2O_3, (this being approximately true for samples held in air). Some compositions were equilibrated at a lower oxygen fugacity at which FeO predominates over Fe_2O_3 and these are considered in Section 4.3. The data appear in Tables III and IV and one or two samples are selectively discussed and plotted below in a manner which can be applied to the rest of data.

4.1. The high SiO_2 to high Al_2O_3 series in air

4.1.1. Sample 7K

A visual representation of the effect of temperature on the solubilities of CaO, SiO_2, Al_2O_3, Cr_2O_3 (and Fe_2O_3 which is an impurity in this sample) in crystalline periclase is shown in Fig. 4, in which the two apices of the triangle A show the SiO_2 and CaO contents of the periclase and the third apex would be the R_2O_3 content, except that in place of a third apex there is a triangle B which shows the Cr_2O_3, Al_2O_3 and Fe_2O_3 contents of the periclase solid solutions.

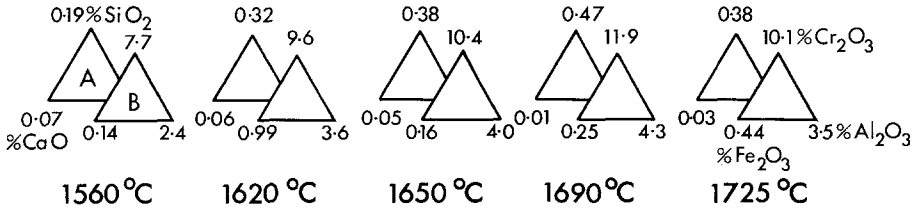

Figure 4 Visual representation of CaO and SiO_2 contents (apices of triangle A) and of Cr_2O_3, Fe_2O_3 and Al_2O_3 contents (apices of triangle B) of periclase solid solutions in sample 7K at various temperatures.

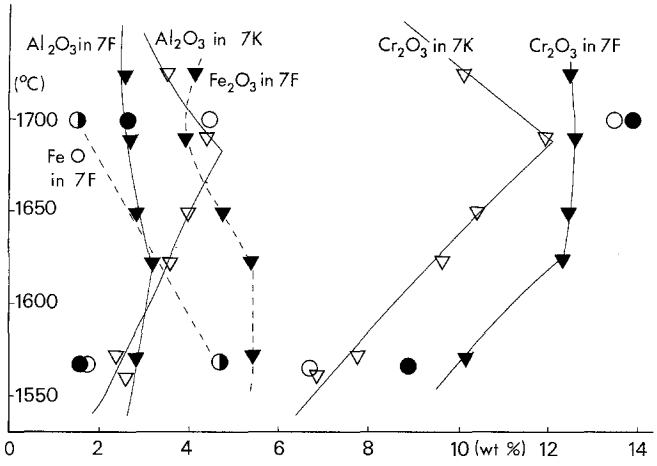

Figure 5 A plot of Al_2O_3 and Cr_2O_3 contents of periclase solid solution in samples 7K ▽, and 7F ▼ (a dashed curve for Fe_2O_3 also shown), versus temperature with curves showing changes of gradient corresponding to changes in the phases present. Also shown, ○, ●, are data for the same samples equilibrated at low fO_2 (dashed curve for FeO) (see Section 4.3).

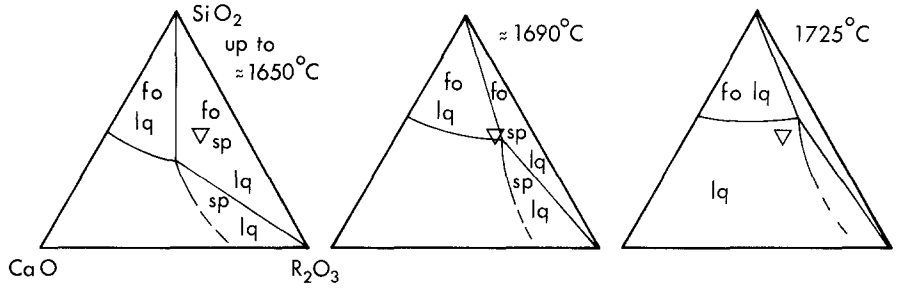

Figure 6 Projection from MgO on to $CaO–R_2O_3–SiO_2$ of sample 7K (the triangle) and the phase fields in which it lies (periclase also present in all fields). Periclase, forsterite, spinel and liquid are present to above 1650° C (Table III) and periclase, forsterite and liquid to above 1690° C. By 1725° C only periclase and liquid are present.

A second diagram (Fig. 5) shows some of the same data (open triangles) as a plot of the Al_2O_3 and Cr_2O_3 contents of periclase solid solution versus temperature. To explain the break in the curves at 1680° C requires an understanding of the phase equilibrium behaviour of the sample which is illustrated in Fig. 6. Up to 1650° C and a little higher (Fig. 6a), data for this sample determine the locus of the apex of the periclase solid solution polyhedron at which the spinel, forsterite, and liquid faces meet which is equivalent to point Q in Fig. 2d. When spinel dissolves at about 1680° C the data then refer to a point of the forsterite–liquid edge of the polyhedron and the periclase compositions have a lower R_2O_3 content which results in the breaks in the curves in Fig. 5. In this particular composition, 7K, forsterite dissolves at some temperature above 1690° C and the percilase solid solution then lies somewhere on the liquid face.

4.1.2. Sample 7F

Plots of the Al_2O_3, Fe_2O_3 and Cr_2O_3 contents of periclase solid solutions for this sample are shown

in Fig. 5. The break at about 1620° C corresponds to the disappearance of spinel as temperature is raised. With this and other iron-bearing samples however, there is the added complication that increasing temperature converts Fe_2O_3 to FeO. Unfortunately, only total iron is determined by probe analyses. Thus in Fig. 5 there will be different amounts of Fe^{2+} replacing Mg^{2+} at each temperature and this change may also influence the solubility of Cr_2O_3 which is greater than expected in this sample, (i.e. it does not decrease after spinel ceases to be stable at 1620° C).

4.2. Chemistry of periclase solid solutions

Data for all samples are given in Table III and the following chemical trends were noted.

Cr_2O_3 solubility in terms of wt% increases with temperature, 16.0% being the highest level encountered. In general, samples containing R_2O_3 composed of $Al_2O_3 + Cr_2O_3$ had 2 to 3 wt% less Cr_2O_3 in the periclase solid solution than those containing $Al_2O_3 + Cr_2O_3 + Fe_2O_3$, (e.g. Fig. 5) thus the presence of iron (replacing its molar equivalent of Al_2O_3 in the bulk sample) increases the solubility of Cr_2O_3 in the periclase. There were

TABLE III Analyses of periclase in the system $CaO–MgO–Al_2O_3–Cr_2O_3–Fe_2O_3–SiO_2$ in air

Comp.	(°C)	SiO_2	Al_2O_3	Cr_2O_3	Fe_2O_3	CaO	MgO	Total	Others
7K	1725	0.38	3.50	10.06	0.49	0.03	85.55	100.01	None
7K	1690	0.47	4.34	11.89	0.25	0.01	83.25	100.22	Fo
7K	1650	0.38	3.98	10.39	0.18	0.05	85.46	100.44	Sp, Fo
7K	1620	0.32	3.56	9.56	0.99	0.06	86.03	100.50	Sp, Fo
7K	1570	0.26	2.33	7.72	0.24	0.04	89.93	100.51	Sp, Fo
7K	1560	0.19	2.54	6.79	0.14	0.07	90.31	100.04	Sp, Fo
4K	1725	0.37	5.45	12.29	0.47	0.05	81.43	100.06	Sp
4K	1650	0.38	3.77	11.00	0.51	0.05	84.10	99.87	Sp
4K	1570	0.20	2.31	7.22	0.35	0.04	90.18	100.30	Sp, Fo
4K	1570	0.19	2.36	7.03	0.09	0.07	90.78	100.53	Sp, Fo
6K	1725	0.03	4.95	12.73	0.42	0.27	82.07	100.45	Sp
6K	1570	0.10	2.28	7.20	0.21	0.03	90.07	99.88	Sp
6K	1570	0.04	2.21	6.97	0.08	0.05	90.40	99.75	Sp
9K	1725	0.01	5.09	12.77	0.61	0.39	81.57	100.44	Sp
9K	1650	0.00	3.55	9.34	0.14	0.30	86.17	99.50	Sp
9K	1650	0.01	3.48	10.46	0.11	0.32	85.39	99.77	Sp
9K	1570	0.04	2.21	6.97	0.08	0.05	90.40	99.75	Sp
7F	1725	0.62	2.53	12.49	4.61	0.04	80.07	100.36	Fo
7F	1690	0.59	2.65	12.59	4.31	0.03	80.21	100.37	Fo
7F	1650	0.58	2.83	12.49	5.26	0.07	79.22	100.42	Fo
7F	1620	0.58	3.13	12.33	6.00	0.07	78.45	100.55	Sp, Fo
7F	1570	0.41	2.76	10.18	6.10	0.02	81.03	100.50	Sp, Fo
4F	1725	0.67	4.14	16.03	6.75	0.10	73.35	101.04	Sp
4F	1650	0.58	3.38	14.03	7.28	0.06	74.74	100.07	Sp
4F	1570	0.45	3.18	10.00	7.80	0.01	79.80	101.24	Sp, Fo
6F	1725	0.13	4.36	15.35	6.92	0.31	73.84	100.90	Sp
6F	1650	0.05	3.47	12.83	6.65	0.32	76.74	100.06	Sp
6F	1570	0.33	2.69	10.48	7.07	0.03	80.70	101.30	Sp
9F	1725	0.05	3.85	13.76	6.37	0.46	76.01	100.50	None
9F	1650	0.03	3.36	12.88	6.65	0.46	76.03	99.38	Sp
9F	1570	0.04	2.60	9.93	6.83	0.13	81.51	101.04	Sp
8K	1690	0.01	0.18	0.64	0.04	1.31	98.16	100.34	L, plus
8K	1620	0.00	0.18	0.53	0.18	1.05	98.43	100.37	L, plus
8F	1690	0.00	0.11	0.61	0.46	1.23	97.52	100.35	L, plus
8F	1620	0.01	0.13	0.53	0.42	0.98	97.93	99.99	L, plus
16F	1560	0.02	0.14	0.48	0.57	0.85	98.65	100.71	Plus
24K	1620	0.01	0.20	0.45	0.00	0.87	98.11	99.65	Plus
24K	1560	0.00	0.24	0.44	0.02	0.77	98.28	99.73	Plus
24F	1690	0.01	0.10	0.52	0.43	1.17	97.64	99.87	None
24F	1620	0.00	0.14	0.49	0.52	0.92	98.05	100.11	Plus

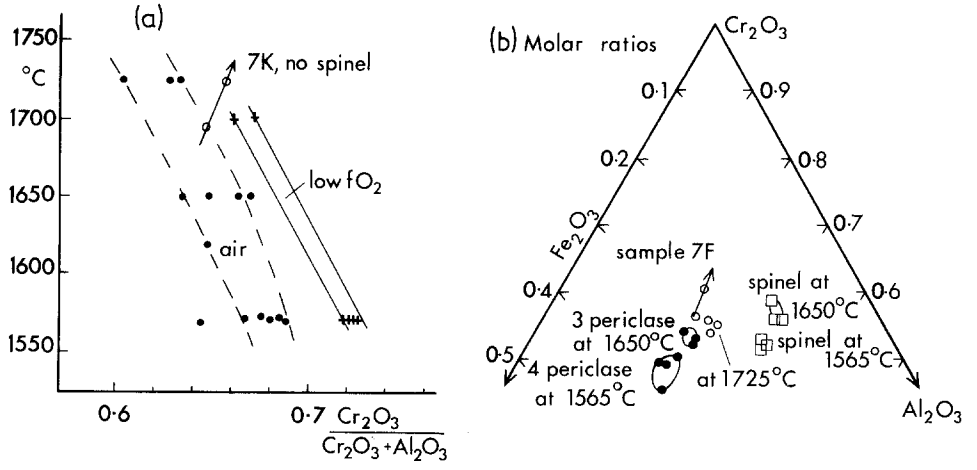

Figure 7 (a) $Cr_2O_3/(Cr_2O_3 + Al_2O_3)$ molar ratios for periclase solid solutions from the high-SiO_2 and high-Al_2O_3 series (for samples held in air and at low fO_2) plotted versus temperature. (b) Molar distribution of Cr_2O_3, Fe_2O_3 and Al_2O_3 in periclase solid solutions and in spinel, with the effects of temperature noted.

regular changes with temperature of the molar ratio Cr_2O_3/R_2O_3 (Fig. 7a). When only Cr_2O_3 and Al_2O_3 were present, Cr_2O_3 was favoured at lower temperatures (ratio 0.68), *falling* with rising temperature to 0.62 at 1725° C. In other words the rate of increase of Al_2O_3 solubility with temperature was greater than that of Cr_2O_3 solubility. When Cr_2O_3 and iron and Al_2O_3 were present, however, Cr_2O_3 was a lesser fraction of the R_2O_3 group (ratio 0.50 at 1565° C, Fig. 7b) and in this case *rising* to 0.55 at 1725° C due presumably to an enchanced solubility of Cr_2O_3 when more Fe^{2+} is present.

Al_2O_3 and Fe_2O_3 solubility. Samples with Cr_2O_3 present (e.g. 7K) in general have about 1 wt% more Al_2O_3 than the Cr_2O_3-free samples (e.g. 7A), thus the presence of Cr_2O_3 appears to change the periclase structure to enchance the solubility of Al_2O_3. The presence of iron seems to have the reverse effect but the data are scarcely adequate to consider this proved. The solubility of iron itself decreases slightly with increasing temperature (Table III).

SiO_2 solubility is very low or undetectable in the more aluminous samples (6K, 6F and 9K, 9F, Table III). It was also low in the CaO–MgO–Al_2O_3–SiO_2 system (Table II). Detectable levels and increasing levels with increasing temperature were noted for samples 4K and 7K (up to about 0.40%) and even greater values for 4F and 7F (about 0.65%). There is a genuine increase in solubility with temperature of Si^{4+} in MgO, when Cr_2O_3 is present in the structure.

CaO solubility is low in silica-rich samples and reaches its highest levels (0.46%) in the CaO-rich, iron-bearing sample 9F.

4.3. Results at low fO_2

Preliminary experiments at 1565 and 1700° C on selected samples (Table IV) were made using a CO/CO_2 gas mixture to control the oxygen pressure to a little below that at which iron metal oxidizes to FeO (about 10^{-9} atm at 1565° C and 10^{-8} atm at 1700° C). As a result most of the iron in most of the samples will be Fe^{2+} with very little Fe^{3+}, the chromium which in air was present as Cr^{3+} with some Cr^{6+}, will become Cr^{3+} with perhaps some Cr^{2+}.

The chemical trends in the periclase solid solutions which are of note are (i) there is about 1 to 2 wt% more Cr_2O_3 in the periclase than in the equivalent runs in air; (ii) Al_2O_3 contents are the same or lower at low fO_2 than they were in air; (ii) iron shows a considerable variation and comparison with samples held in air is not justifiable because Fe^{3+} is a significant species dissolving when air is used but Fe^{2+} predominates when low fO_2 is used. At low fO_2, the temperature effect is such that about 5% FeO dissolves in the SiO_2-rich samples and 9% in the Al_2O_3-rich samples at 1565° C but the levels fall to below 2% at 1700° C. These features indicate that at 1565° C, alternative oxidation and reduction of a sample leads to little change of iron distribution between phases (presumably within periclase Fe^{2+} moves to a nearby site when it is converted to Fe^{3+}). At 1700° C,

TABLE IV Probe analyses of periclase in the system $CaO-MgO-Al_2O_3-Cr_2O_3-FeO-SiO_2$ from samples equilibrated at low fO_2

Comp.	(°C)	SiO_2	Al_2O_3	Cr_2O_3	FeO	CaO	MgO	Total	Others
7K	1700	0.48	4.42	13.41	0.27	0.04	81.87	100.49	Fo
7K	1565	0.11	1.71	6.61	1.80	0.04	90.42	100.69	Fo, Sp
7K	1565	0.13	1.67	6.54	2.13	0.05	90.00	100.51	Fo, Sp
9K	1700	0.02	4.57	13.22	0.99	0.26	81.37	100.43	Sp
9K	1565	0.00	2.18	8.44	1.00	0.31	88.23	100.16	Sp
9K	1565	0.00	2.18	8.48	1.60	0.34	87.52	100.12	Sp
7F	1700	0.44	2.59	13.81	1.67	0.05	81.58	100.14	Fo
7F	1565	0.19	1.54	8.82	4.78	0.05	83.80	99.18	Fo, Sp
4F	1700	0.54	3.80	17.10	1.50	0.06	77.82	100.82	None
4F	1565	0.33	2.03	11.16	5.11	0.10	81.98	100.71	Sp, Fo
6F	1700	0.08	3.61	15.92	1.31	0.18	79.66	100.75	None
6F	1565	0.00	1.93	10.39	6.35	0.26	81.98	100.91	Sp
9F	1700	0.00	3.37	17.15	1.96	0.58	77.47	100.54	Sp
9F	1565	0.00	1.19	8.66	8.73	0.57	81.92	101.06	Sp
9F	1565	0.00	1.18	8.29	9.01	0.52	81.76	100.75	Sp
8K	1565	0.00	0.40	6.77	0.25	1.24	89.52	98.19	Plus

however, reduction does drive much of the iron out of the periclase and oxidation will cause it to re-enter the periclase.

4.4. The high-CaO series

Samples with CaO present in great excess over the levels of SiO_2 and Al_2O_3 (Fig. 1b) contain periclase solid solutions characterized by very low R_2O_3 contents (Cr_2O_3 0.7% Al_2O_3 0.2% Fe_2O_3 0.5%). Data are presented in the tables and some observed chemical trends are (i) CaO levels depend on temperature and are higher in Sample 8, in which lime is stable, than in other samples with C_2S stable. (ii) Cr_2O_3 levels are low (0.44 to 0.64 wt% Cr_2O_3) but even within these narrower limits the Cr_2O_3 content increases with temperature. (iii) When iron is added to replace Al_2O_3 it dissolves in the periclase without much affecting the levels of Al_2O_3 and Cr_2O_3 present thus the total R_2O_3 dissolved in the periclase is increased even although the total molar R_2O_3 in the starting composition has not been changed.

Under reducing conditions, at an oxygen pressure of about 10^{-9} at 1565° C the high-CaO series corroded the molybdenum support wires very quickly, but two samples survived and show a very enchanced solubility of chromium in periclase (up to 6.8% Cr_2O_3).

The enhanced solubility of chromium at low fO_2 is a reflection of the equilibrium $2CrO_3 \rightleftharpoons Cr_2O_3 + \frac{3}{2}O_2$ being displaced to the right, relative to its position when the sample is held in air. Or, alternatively, one can think of the lime-rich samples (when held in air) containing relatively high levels of Cr^{6+} which is apparently not soluble in periclase.

This enormous change in the chromium content of periclase solid solutions with changing fO_2 is likely to be a factor in the development of the equilibrium texture of chrome-bearing bricks in high-lime environments, notably in cement kilns, if subjected to a lower fO_2 than that at which the brick was made.

4.5. Reversibility of equilibria

Some experiments were made to test the reversibility of the equilibria. The material quenched from about 1700° C (composed of periclase crystals up to 200 μm enclosed in glass) was reloaded in a new capsule and raised to 1560° C and held for 19 h. After quenching the product was composed of large periclase crystals with a clear rim of up to 40 μm and a centre zone of periclase laden with exsolved spinel. Microprobe analyses of the clear periclase rim gave values of Cr_2O_3 and Al_2O_3 quite close (within a factor of 0.9 to 1.0) to the values previously found by direct heating of finely ground starting materials to 1560° C but Fe_2O_3 levels were different, being lower (by a factor of about 0.67) than in direct heating-up runs.

The texture of exsolved spinel found at the core of the periclase crystals is a texture commonly developed in commerical refractories [8].

4.6. Other phases analysed

The experiments were designed to determine the behaviour of periclase solid solutions but random

TABLE V Probe analyses of spinel

Comp.	(°C)	SiO_2	Al_2O_3	Cr_2O_3	FeO*	CaO	MgO	Total
7K	1650	0.33	33.08	41.95	0.20	0.16	25.28	100.99
4K	1725	0.22	32.15	42.07	0.44	0.13	24.81	99.83
4K	1650	0.15	30.64	43.53	0.62	0.25	24.55	99.74
4K	1570	0.18	32.54	41.78	0.77	0.15	24.82	100.23
4K	1570	0.16	34.43	39.03	0.90	0.18	25.00	99.69
6K	1725	0.00	32.53	42.75	0.21	0.29	24.82	100.61
9K	1725	0.00	31.53	42.73	0.72	0.51	24.29	99.79
9K	1650	0.00	34.77	39.32	0.59	0.60	24.00	99.27
4F	1650	0.19	17.10	45.97	10.65	0.24	25.85	99.99
4F	1570	0.16	17.31	44.20	13.23	0.18	22.47	98.55
6F	1650	0.00	17.38	47.99	10.31	0.46	22.41	98.55
6F	1570	0.07	16.92	44.46	14.16	0.15	23.13	98.87
9F	1650	0.00	15.60	48.06	9.85	0.86	23.57	97.94
9F	1570	0.05	16.08	41.68	13.84	0.58	23.01	95.25
9F	1700	0.09	18.92	56.49	0.87	1.02	19.11	96.50

*Iron reported as FeO but probably substantially present as Fe_2O_3.

analyses of spinels were made (Table V), and some of the chemical trends noted were; (i) very little change in spinel composition as other variables changed. When only Cr_2O_3 and Al_2O_3 were present the spinels had $Cr_2O_3/(Cr_2O_3 + Al_2O_3)$ ratios of 0.43 to 0.48 showing that relative to the starting material Al_2O_3 is slightly concentrated in the spinels relative to Cr_2O_3. When Cr_2O_3, Al_2O_3 and iron were present (the data are shown in Fig. 7b) Cr_2O_3 was about 55 mol% of the R_2O_3 group, Al_2O_3 about 30% and Fe_2O_3 about 15% thus iron was preferentially rejected from the spinel and presumably somewhat concentrated in the liquid; (ii) CaO levels where up to 0.9% in spinels from CaO-rich iron-bearing samples; (iii) FeO levels decrease with increasing temperature.

Only one spinel from a sample held at low fO_2 (at 1700° C) was analysed; it showed a chemistry different from that of the spinels formed in air, being richer in Cr_2O_3 (56.5%) and very low in iron (0.9 wt%) and with the highest CaO content encountered (1.0%).

5. Derived diagrams and applications

As is inevitable in a seven component system, critical data are hard to come by but some notion of the chemistry of the periclase solid-solution polyhedron is obtainable from the present random data which can be replotted in a variety of ways of which a few examples are given here.

A plot of the data of 1725° C (Fig. 8) shows part of the locus of the spinel to liquid edge of the polyhdedron and demonstrates its movement to lower R_2O_3 content as the CaO content of the bulk composition increases. Any CaO contamination of a brick in service will drive R_2O_3 out of the periclase crystals.

Changes in the relative molar solubilities of Al_2O_3, Cr_2O_3 and Fe_2O_3 are shown in Fig. 7. For samples containing R_2O_3 composed of Cr_2O_3 + Al_2O_3 (Fig. 7a) the variation is not great (in contrast with the great range in wt% of Al_2O_3, Cr_2O_3 and Fe_2O_3 shown in Fig. 5) but samples held in air fall in a distinctly different zone from those held at low fO_2. Two of the samples from composition 7K differ from the others in not having spinel present in the equilibrium assemblage and these two show a contrasted behaviour. For the majority, the slope is in the sense of a relative enrichment in Al_2O_3 with increasing temperature. Fig. 7b shows molar ratios of the Cr_2O_3, Fe_2O_3 and Al_2O_3 contents of periclase and of spinel solid solutions. The behaviour of periclase solid solutions with spinel present in the equilibrium assemblage is towards increasing Cr_2O_3 content and decreasing iron content as temperature rises. Sample 7F does not have spinel in the equilibrium assemblage at

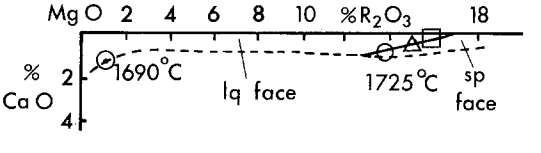

Figure 8 Data from 1725° C used to construct part of the locus along which the spinel and liquid faces of the periclase polyhedron meet (compare Fig. 2a), in the system with R_2O_3 composed for Cr_2O_3, Al_2O_3 and iron (with one CaO-rich sample at 1690° C, see Section 4.4 to locate approximately another region of the polyhedron).

1650 and 1725° C and the locus of its periclase solid solutions is shown.

There are insufficient samples from the high CaO series to determine a trend, but the periclase solid solution from sample 8K when held at low fO_2 had a large ratio of $Cr_2O_3/(Cr_2O_3 + Al_2O_3)$ of 0.9, well to the right of the scale in Fig. 7a.

The increasing solubility of Cr_2O_3 in periclase with increasing temperature reduces the compositonal volume within which spinel crystallizes which, in turn, changes the proportion of phases present in refractory compositions. Fig. 9 is a simplified illustration in which, to keep it in two dimensions, data have been projected from CaO on to $MgO–Al_2O_3–SiO_2$ and liquid is present in all assemblages. A composition such as V at low temperature (about 1550° C) is composed of Fo, Sp and P_{14} (where P is periclase and the subscript numeral is the approximate R_2O_3 content calculated as if it were Al_2O_3). At a higher temperature, such compositions are composed of Fo, P_{19}, and liquid, having lost spinel (and any extra-bonding effects due to the presence of spinel). Other compositions, such as W (which are compounded with more chromite) ensure that spinel is present at higher temperature, but the amount of spinel present changes markedly with temperature. As drawn in Fig. 9 the percent of spinel in composition W decreases from 22% at 1550° C to 15% at 1700° C, but more interestingly, and perhaps of more importance, the amount of periclase in the sample W actually increases from 66% at 1550° C to 72% at 1700° C. This increase is a form of retrograde solubility, and could perhaps in practice be a means of forming bonds between adjacent periclase crystals, if the extra crystalline periclase can be induced to grow on existing crystals, rather than to form new nucleii.

The maximum R_2O_3 content of periclase solid solution most probably is found at the 'break' in the curves shown in Fig. 5 and it would seem from the photographs and comments of Landy [8] that there may be technological advantages in creating a microstructure with precipitated spinel in the periclase crystals. To obtain the maximum precipitation of spinel would require controlled heating of the chosen refractory composition to just attain the temperature appropriate to the maximum solubility, or, if heating to a higher temperature was required for other reasons, then the cooling period at the temperature of maximum solubility should be long enough to allow the chemicals to reach the maximum solubility.

6. Final remarks

The pattern of solubility of CaO, Al_2O_3, Cr_2O_3 (and an initial ideal of the behaviour of $FeO–Fe_2O_3$) is clear. The literature values for the solubilities of CaO, Al_2O_3 and Cr_2O_3 in their appropriate binary systems are in general different from their solubilities when *all* are present. The presence of other crystalline phases constrains the periclase composition such that it lies on faces, edges or apices of the periclase solid solution polyhedron. When the geometry of the polyhedron is known it can be used to predict periclase compositions. The rational behaviour of the Fe_2O_3, Al_2O_3 and Cr_2O_3 contents of periclase solid solutions in response to temperature and the presence of other phases allows a conscious choice to be made in refractory formulations as to which phases are wanted and in what *relative* proportions at the working temperature of the refactory. The final key is to obtain the liquid composition, which has so far only been partially accomplished in $CaO–MgO–Al_2O_3–SiO_2$ (Fig. 3). If successful in systems containing Fe_2O_3 and Cr_2O_3 it would allow *absolute* calculation of the proportions of phases present.

The extent of Al_2O_3, Fe_2O_3 and Cr_2O_3 solu-

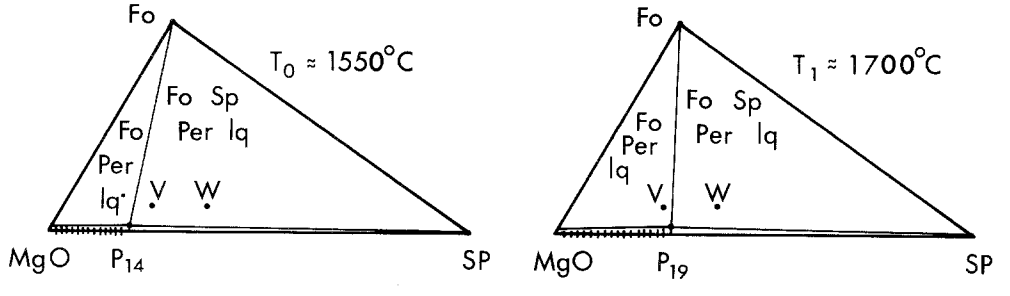

Figure 9 Projection from CaO into a part of the plane $MgO–SiO_2–Al_2O_3$ to illustrate the change in proportions of phases as temperature changes.

bility is such that there are compositions with as much as 3.4% Al_2O_3. 6.7% Fe_2O_3 and 12.9% Cr_2O_3 and as little as 76% MgO which are solid at 1725° C. In any commercial composition approaching this the presence of impurity CaO in excess of 0.5% and of SiO_2 generates a liquid. Such compositions, at a working face temperature of 1725° C, are composed of periclase (±liquid) but the cooler zones of the brick will contain spinel (e.g. composition V, Fig. 9).

Iron and its alternate oxidation and reduction is often blamed for bursting of refractories as it dissolves and exsolves in periclase. The data in the tables and figures show that with temperature changes there is a greater movement of chromium in and out of periclase than there is of iron (when the samples are equilibrated in air).

References

1. G. M. BIGGAR, *J. Australian Ceram. Soc.* **11** (1975) 9.
2. D. C. PRESNALL and N. L. BRENNER, *Geochim. Cosmochim. Acta* **38** (1974) 1785.
3. G. M. BIGGAR and M. J. O'HARA, *Mineral. Mag.* **37** (1969) 198.
4. *Idem, Progress in Experimental Petrology,* Series D No. 2 (Natural Environment Research Council, London, 1972).
5. G. M. BIGGAR, *Refractories J.* **47** (1972) 6.
6. M. J. O'HARA and G. M. BIGGAR, *Trans. Brit. Ceram. Soc.* **69** (1970) 243.
7. R. G. CAWTHORN, C. E. FORD, G. M. BIGGAR and M. S. BRAVO, *Earth and Planet. Sci. Lett.* **21** (1973) 1.
8. R. A. LANDY, *Industrial Heating* **42** (1975) 63.

Received 28 January and accepted 20 April 1977.